Accuracy and metal removal analysis in orbital electrochemical hole sizing

Essam Soliman
Production Eng. Dept., Faculty of Eng., Alexandria University, Alexandria, Egypt
e_soliman@alex.edu.eg

This work provides an accuracy and metal removal analysis of the orbital electrochemical hole sizing process. A process model that considers both feeding and non feeding tools is developed. The model correlates process variables and parameters and process performance measures. Process variables are time dependent; they include rotational speeds of tool and work part and tool feedrate. Process parameters are time independent; they include tool radius and tool lip height. Performance measures of the process include specific cutting energy, volumetric and linear removal rates and average roundness and straightness errors. Model Simulations showed that the specific cutting energy of the process is independent of process parameters, and its value is much larger compared with those for conventional machining operations. Simulation results, also, showed that rotations of the tool and the work part do not affect any of the process performance measures. However, increasing tool radius, feedrate and tool lip height proved to increase volumetric and linear removal rates, and to decrease average straightness error. Increasing tool radius and feedrate reduced hole average roundness error while increasing tool lip height increased it.

تقدم هذه الورقة البحثية تحليلاً لمعدلات إزالة المعدن ودقة عملية الضبط الكهروكيميائي للثقوب. يعتمد التحليل على بناء نموذج رياضي لعملية القطع باستخدام أدوات قطع بتغذية وبدون تغذية . متغيرات النموذج الرياضي تتغير مع زمن التشغيل ويمكن استخدامها للتحكم في عملية القطع . عناصر النموذج الرياضي ثابتة ولا تتغير مع زمن التشغيل . يربط النموذج الرياضي بين المتغيرات والعناصر من جهة وبين مقاييس الأداء لعملية الضبط من جهه اخرى. تشمل المتغيرات سرعات دوران الأداة والشغلة وسرعة تغذية الأداة ومقدار انحراف الأداة عن محورها أثناء الدوران . تشمل العناصر قطر وسمك الأداة وانحراف الشغلة عن محورها أثناء الدوران . تشمل مقاييس الأداء معدلات إزالة المعدن الخطية والطولية ودورانية السطح واستوائيتة وكذلك الطاقة النوعية للقطع . تم عمل نموذج محاكاة على الحاسب وأوضحت نتائج المحاكاة أن سرعات الدوران للشغلة والأداة لا تؤثر على أداء عملية القطع من الناحية النظرية . لكن زيادة كل من قطر الأداة وارتفاعها ومعدل التغذية يزيد معدلات إزالة المعدن ويقلل من عدم استوائية السطح . زيادة كل من القطر ومعدل التغذية يقلل من عدم دورانية السطح في حين أن زيادة سمك الأداة يزيده . الطاقة النوعية للقطع ثابته ولا تتغير بتغير متغيرات وعناصر عمليه القطع.

Keywords: Orbital electrochemical sizing, Modeling and simulation, Process Characterization

1. Introduction

Electrochemical Machining (ECM) covers a wide range of machining processes, in which material is removed by electrolytic dissolution of an anodic work part. A cathode tool, with a predefined form, is fed towards and/or along work part surface, to adjust its geometry. An electrolyte fills the gap between the tool and work part. Among the advantages of ECM is its ability to machine very hard and difficult to machine materials at high removal rates. Also, electrochemical machined surfaces are free from burr and thermal and residual stresses and have good surface finish. Industrial applications of ECM include auto-body dies, plastic molds and turbine blades. Electrochemical Drilling (ECD) is a major class of ECM. Research work has shown that ECD processes are superior to other non-conventional drilling operations [1-2], especially when their operational parameters are properly adjusted. Orbital Electrochemical Drilling (OECD) is a special ECD process in which an

eccentric rotating tool is feed onto a work part to open a through or blind hole in it. Orbital Electrochemical Sizing (OECS) is a complementary process used to enlarge a hole, produced by ECD or any other drilling process, and/or to adjust its size.

J. Kozak et al. [3-4] developed a 2-D model for ECM. The model considered a general form moving and rotating electrode tool. Work part form variations, during machining, were obtained via simulated changes in a quasi-envelope. Simulation software was very efficient in optimizing machining parameters. However, the work part was assumed immovable. Therefore, the model is not suitable for simulating the general OECS process wherein both work part and tool move. H. Hardisty et al. [5] developed a 2-D model and finite element simulation of ECM. Theoretical and finite element simulation results were in good agreement. However, the model was restricted to a feeding/stationary electrode and a flat stationary work part. M. Purear et al. [6] developed a 3-D finite element model for ECM. The work part was stationary while the electrode was fed in one direction to machine an indentation in a flat surface. The developed model was not expensive in computational time. However, the model was not tested for the case where both the electrode and work part move in more than one direction.

H. Hocheng et al. [7-8] developed a model for simulating the development of an eroded opening during electrochemical boring of a hole. Both of the cylindrical electrode tool and the work part were stationary. Authors reported good agreement between experimental and simulations results. However, the flat bottom surface of the electrode represented the only active surface of the tool. The cylindrical surface of the electrode did not take part in machining, which is not the case for the OECS process. X. Jiawen et al. [9] developed a model for contour evolution machining using a rotary tool electrode. The electrode was assumed to run true around its geometric center. Feed direction of the electrode was parallel to the machined surface. No relative displacement took place between the electrode and the work part in the direction of the electrode axis. Considerable refinement of the model is needed so that it can be applied to the OECS process.

M. S. Hewidy et al. [10] developed a model for the electrochemical drilling under orbital motion conditions. The electrode was a tube with isolated cylindrical surface. Only the bottom of the tube took part in machining. The authors designed an experimental set up to verify their model. Experimental and model simulation results were in good agreement. Results showed that using orbital motion enhances the accuracy of the machined hole. Rajurkar, K.P. et al. [11] showed, experimentally, that the performance of electrochemical hole drilling process can be improved by using orbiting electrode tool. They also showed that current spikes due to debris accumulation in the gap diminished resulting in better surface finish. H. El-Hofy et al. [12-13] conducted experimental work to study the effect of different machining parameters on quality of holes produced by the OECS process. They used both feeding and non-feeding disc like electrode tools. The parameters included tool lip height and feedrate. They concluded that using orbiting tools results in good surface finish, low roundness errors and efficient machining.

E. Soliman et al. [14-15] developed a simulation model for the OECS process. An eccentric rotating disc like electrode tool was fed along the axis of a hole in a work part. The electrolytic action was assumed to take place around the tool periphery. Experimental work was used to check model validity. Some deviations between simulations and experimental results were reported. In fact, these deviations stimulated the present work which adopts a new methodology for modeling and simulating the OECS process.

2. Process model

The model considers a cylindrical hollow work part of height h_w and initial mean radius $\overline{R}_w$ as shown in fig. 1. The geometric center of the work part is *B*. The work part rotates at a speed of N_w around the set up center *D*, which represents work part fixture center. Possible error in work part set up is represented by work part eccentricity e_w. An electrode tool of

height h_t and a circular cross section of radius R_t is fed through the work part at a rate of f. Two tools are used; Tool (1) is a disc like tool with $h_t < h_w$, while Tool (2) is a cylindrical tool with $h_t \geq h_w$. Tool (1) is a feeding tool, $f > 0$, while Tool (2) is a non-feeding one, $f = 0$. The geometric center of the tool is C. The tool rotates at a speed of N_t around the center A. Tool eccentricity e_t is deliberately added to machining set up in order to create the orbital motion of the tool. The eccentricity between A and D is referred to set up eccentricity e_s. It is the distance between the center of rotation of the work part fixture and that of the tool fixture. In the present work, small radius pilot tools are employed. The radius of the tool is less than one half of that of the work part. Such tools require small power supply as less machining current is needed. Also, current density is relatively high leading to good hole surface finish. The rotational speeds, N_w, and N_t, feedrate f, and eccentricity e_t are arbitrary functions of time, t, and therefore, are considered as process variables. On the other hand, h_w, h_t, R_t, e_s, and e_w are time independent and therefore are considered process parameters.

The work part is modeled as a stack of J thin discs each of height h; $h_w = J \times h$. Each disc is further divided into K radial sectors. The radius of the hole is then represented by the matrix $R_w(j,k)$. The index j, $j = 1$ to J, represents an arbitrary disc while index k, $k = 1$ to K, represents an arbitrary sector within the disc j. The mean radius of the work part at any time during machining is $\overline{R}_w$ and is obtained by averaging the elements of the matrix $R_w(j,k)$. Therefore,

$$\overline{R}_w = \frac{1}{J \cdot K} \sum_{j=1}^{J} \sum_{k=1}^{K} R_w(j,k). \quad (1)$$

In eq. (1), the matrix $R_w(j,k)$ and consequently $\overline{R}_w$ varies over time. Their values at $t = 0$ represent the initial geometry of the hole which depends on the preceding machining operations. Each tool is represented by a stack of L thin discs, each of height h; $h_t = L \times h$. The distance between B and C is the actual or equivalent eccentricity e_q. The angle between BC and AD, φ_q, is the actual or equivalent angular position of the tool, with respect to the geometrical center of work part. The parameters e_q and φ_q are calculated from the following equations:

$$e_q = \sqrt{(e_t \sin\varphi_t - e_w \sin\varphi_w)^2 + (e_s - e_w \cos\varphi_w + e_t \cos\varphi_t)^2}. \quad (2)$$

$$\varphi_q = \tan^{-1} \frac{e_t \sin\varphi_t - e_w \sin\varphi_w}{e_s - e_w \cos\varphi_w + e_t \cos\varphi_t}. \quad (3)$$

Where, φ_t is the angular position of tool, $\varphi_t = 2\pi t N_t$, and φ_w is the angular position of the work part, $\varphi_w = 2\pi t N_w$.

The tool moves from an initial position $x_t = 0$, to a final a position $x_t = T$, where T is total machining time. The final position of the tool is given from the equation:

$$x_{t=T} = \sum_{t=0}^{T} f \cdot \Delta t = h_w + h_t. \quad (4)$$

In eq. (4), Δt represents time step for model simulation. It is selected, in conjunction with h, so that the distance travelled by the tool during Δt is less than h; $\Delta t < h/f$. In case of the cylindrical tool, the tool runs continuously for the period of T.

An electrolyte is pumped to fill the gap between the tool and the work part. Flow rate is assumed to be large enough so that electrolyte conductivity κ is constant and is not considerably affected by heat generated during machining or sludge produced during work part dissolution. The rotation of tool and/or work part helps this assumption to stand true.

A voltage V is applied across the cathode tool and the anode work part. Current is assumed to flow from machining zones of discs of the work part to conducting zones of mating discs of the tool, in radial direction with respect to the work part geometrical center. This ensures that current lines follow minimum paths with minimum resistances.

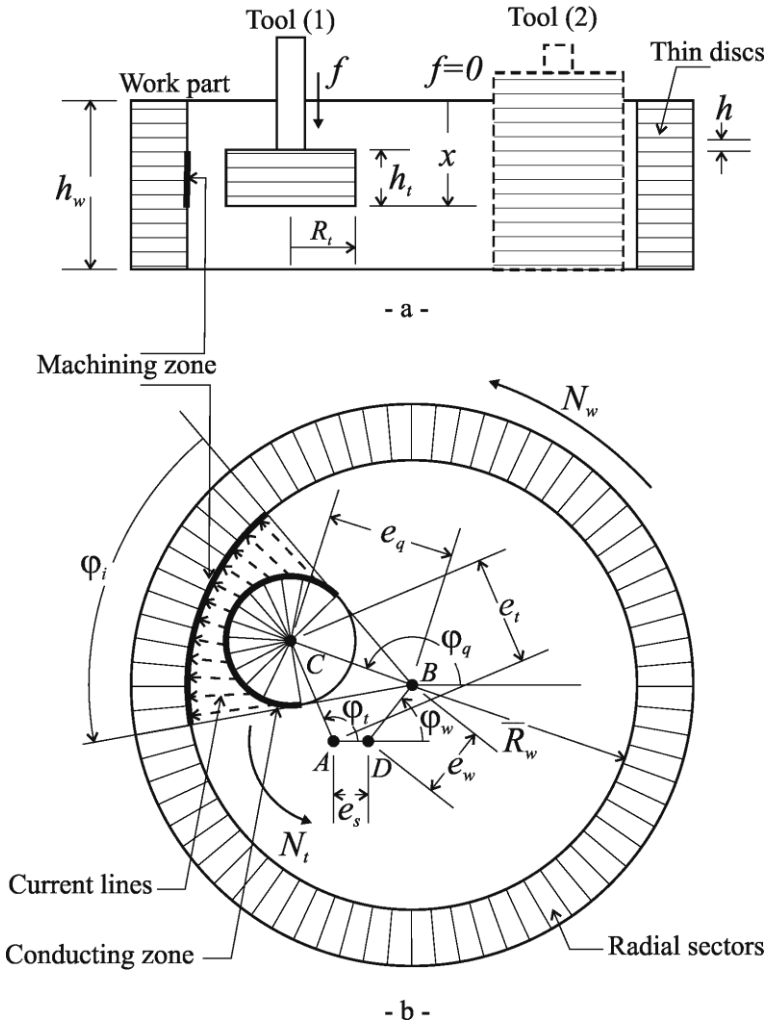

Fig. 1. Model of the orbital electrochemical hole sizing process.

This assumption is basically true at the middle of the conducting zone, where the machining gap is relatively small and current lines are perpendicular to both conducting and machining zones. Near the sides of the machining zone, current lines will not be normal to the tool surface and, therefore, will deflect and widen the machining zone, resulting in an over cut. However, at the sides of the machining zone, the machining gap is relatively large and consequently current density and current efficiency are small. Using an electrolyte such as $NaNO_3$ or an insulator would decrease the effect of such deflected current lines.

Current flows within the included angle φ_i as shown in fig. 1, which depends on tool radius and actual eccentricity. It is given from the equation:

$$\varphi_i = 2\sin^{-1}\frac{R_t}{e_q}. \tag{5}$$

The number of work part sectors subjected to machining within the machining zone of one tool disc, neglecting stray current, is K_m and is calculated from the following equation:

$$K_m = \frac{\varphi_i \cdot K}{2\pi} = \frac{\sin^{-1}\dfrac{R_t}{e_q}}{\dfrac{\pi}{K}}. \tag{6}$$

It is important to notice that even K is an arbitrary parameter, it must be selected so that the relative rotational angle between tool and work part during one time step Δt corresponds to one work part radial sector. This condition is expressed as:

$$K = \frac{n}{(N_w - N_t) \times \Delta t}. \quad (7)$$

Where, n is a positive integer where $n \geq 1$. Large n will lead to accurate simulation results but simulation time will be largely increased.

The gap between the conducting and the machining zones varies within the included angle, φ_i, from one work part radial sector to the other. The work part radial segment index, k_{min}, corresponding to minimum gap, is given from the following equation:

$$k_{min} = \frac{\varphi_q - \varphi_w}{K}. \quad (8)$$

The gap at each radial sector, $g(l,k')$, is determined in the direction of current flow lines using the following equation:

$$g(l,k') = R_w(l,k_{\min} + k' - k_m) - Q(k'). \quad (9)$$

Where,

$$Q(k') = R_t^2 - e_q^2 \times \sin^2 \beta(k') + e_q \times \cos \beta(k'). \quad (10)$$

And,

$$\beta(k') = 0.5\varphi_i - (k' - 0.5) \times \frac{2\pi}{K}. \quad (11)$$

In eqs. (9 – 11), the index k' takes the values from 1 to K_m. These values are mapped to hole radial segments as from $k_{min} - k_m/2$ to $k_{min} + k_m/2$. The index, l, depends on the position of the tool and it varies from l_p to $l_p - L$ where l_p is given by:

$$l_p = \frac{x_{t=t}}{h}. \quad (12)$$

The current, $I(l,k')$, flowing through the gap $g(l,k')$ is given by:

$$I(l,k') = \frac{V \cdot \kappa \cdot K}{2\pi \cdot h \cdot [Q(k') + \frac{g(l,k')}{2}]}. \quad (13)$$

The current density at each work part sector, $I_s(l,k')$, within the machining zone, is then given by:

$$I_s(l,k') = \frac{I(l,k') \cdot K}{2\pi \cdot R_w(l,k_{\min} + k' - k_m) \cdot h}. \quad (14)$$

Total machining current at any time, I_a, is then given by:

$$I_a = \sum_{l=1}^{L} \sum_{k'=1}^{k_m} I(l,k'). \quad (15)$$

The volume of material machined, $v(l,k_{\min} + k' - k_m)$, at the work part sector, $R_w(l,k_{\min} + k' - k_m)$, during Δt, at any time, t, is given from the following basic equation:

$$v(l,k_{\min} + k' - k_m) = \frac{A_w \cdot I(l,k') \cdot \Delta t \cdot \xi}{Z \cdot F \cdot \rho}. \quad (16)$$

Where ξ is current efficiency. The volume of material machined is related to the change in the gap from the following equation, assuming that work part dissolves in radial direction [18]:

$$v(l,k_{\min} + k' - k_m) = \frac{h \cdot \pi}{k_w} \{[R_w(l,k_{\min} + k' - k_m) + g(l,k')]^2 - [R_w(l,k_{\min} + k' - k_m)]^2\}. \quad (17)$$

Therefore, change in gap, $\Delta g(l,k')$, can be given as:

$$\Delta g(l,k') = \sqrt{R_w(l,k_{\min} + k' - k_m)^2 + \frac{v(l,k_{\min} + k' - k_m)}{h \cdot \pi}} - R_w(l, k_{min} + k' - k_m. \quad (18)$$

The radius of the work part, $R_w(l,k_{\min}+k'-k_m)$, at any time can then be given by:

$$R_w(l,k_{\min}+k'-k_m)_{t+\Delta t} = R_w(l,k_{\min}+k'-k_m)_t + \Delta g(l,k'). \quad (19)$$

The total volume removed at any time during machining can be given from the following equation:

$$\upsilon_{a_{t=t}} = \frac{A_w}{Z\cdot F\cdot \rho}\sum_{t=0}^{t}\sum_{l=1}^{L}\sum_{k=1}^{k_m}\xi\cdot I(l,k')\cdot \Delta t. \quad (20)$$

The current efficiency, ξ, is represented by an arbitrary function of current density as, $\xi = f'(I_s)$. The function depends mainly on the type of electrolyte used. The total energy consumed in machining, $W_{t=t}$, at any time, is given from the following equation:

$$W_{t=t} = V\sum_{t=0}^{t} I_a\cdot \Delta t. \quad (21)$$

3. Process characterization

The OECS process is characterized by machining rate, geometrical features of the machined hole and the energy consumed in machining. Machining rate is expressed by rate of change of hole radius, *LRR*, and rate of material removal, *VRR*. They are obtained as overall values, over total machining time, using the following equations:

$$LRR = \frac{\overline{R}_{w_{t=T}}}{T}. \quad (22)$$

$$VRR = \frac{\upsilon_{a_{t=T}}}{T}. \quad (23)$$

They are also obtained for each period of time during machining according to the following equations:

$$LRR_{t=t} = \frac{R_{w_{t=t+\Delta t}} - R_{w_{t=t}}}{\Delta t}. \quad (24)$$

$$VRR_{t=t}\frac{\upsilon_{a_{t=t+\Delta t}} - \upsilon_{a_{t=t}}}{\Delta t}. \quad (25)$$

While eqs. (22 and 23) represent overall machining rates, eqs. (24 and 25) represent incremental rates. Overall rates are easier to measure experimentally while incremental rates provide accurate description of the process characteristics. The parameter *LRR* provides information about how fast hole size is adjusted. It is directly related to *VRR*, which is a common measure of a machining performance, employed in the present work for calculating the specific machining energy as will be explained later.

The geometrical features of the hole include roundness errors of its discs *RE*(*j*) and the straightness error of its sides *SE*(*k*). Roundness errors are averaged to give the average roundness error of the hole, RE_m. Also, straightness errors are averaged to give the average straightness errors of the hole, SE_m. Standard procedures are used for calculating roundness and straightness errors [16].

The energy consumed in machining is expressed by the specific machining energy, W_s, and is obtained by dividing *W* by *VRR*. This is accomplished in two ways; Average W_s is obtained by dividing the total energy consumed during machining by the overall *VRR*, according to the following equation:

$$W_{s_{average}} = \frac{W}{VRR}. \quad (26)$$

Incremental W_s is obtained at any time during machining from the following equation:

$$W_{s_t} = \frac{V\cdot I_a\cdot \Delta t}{VRR_{t=t}}. \quad (27)$$

4. Model simulation

The described model considers several process variables and parameters. Process variables are time dependent while process parameters are time independent. The reason for this discrimination is that process variables can be monitored on line, and therefore, can be used, within a control system, to correct process performance.

Table 1 provides a nomenclature for model variables and parameters as well as their default values used for model simulation. Homogeneity of units is checked before substituting in corresponding equations and correction factors are used whenever necessary.

Process model is simulated using a developed, VC++ programming language based, software. The structure of the software is represented by the flow chart shown in fig. 2. Initial hole geometry and process and simulation parameters are stored in text files. A GUI allows the user to select these files and modify the different parameters.

A module converts the text files data into data structures and stores them in computer memory for further processing. Simulation starts by determining position of the tool and updating tool feedrate in case of using a feeding tool with a variable feedrate. Then, a module determines the indices of the facing discs of the tool and those of the hole. In case of a non-feeding tool, all discs of the hole face discs of the tool. The gaps between the facing discs of the tool and hole are then calculated and used to determine current and material removed at each radial segment at each time step. Hole radius data structure is then updated. Process variables such as current,

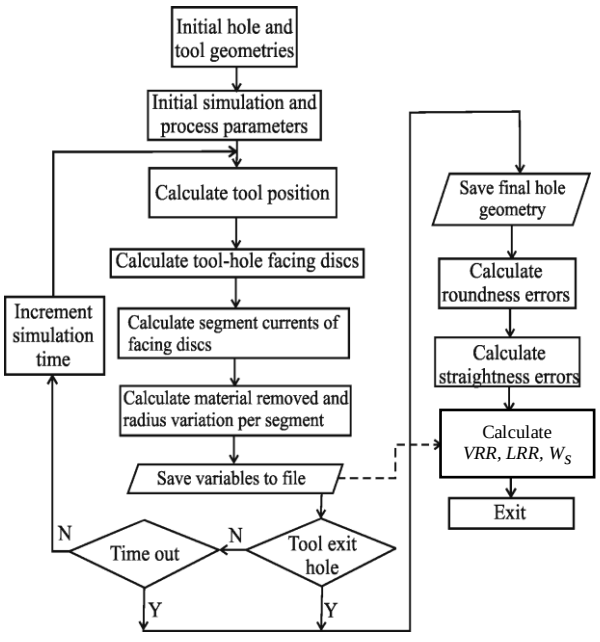

Fig. 2. Flow chart of the simulation software.

Table 1
Nomenclature and default values for variable and simulation parameters

	Parameter	Symbol	Value [unit]
Process parameters	Work part height	h_w	15 [mm]
	Tool radius	R_t	5 [mm]
	Tool (1) height	h_t	15 [mm]
	Tool (2) height	h_t	3 [mm]
	Set up eccentricity	e_s	0 [mm]
	Work part eccentricity	e_w	0 [mm]
	Atomic weight	A_w	56 [Kg/mole]
	Valence	Z_w	2 [ ]
	Density	ρ_w	7800 [Kg/m3]
	Faraday's constant	F_a	96500 [C/mol]
	Conductivity	κ	25 [1/Ω/m]
	Current efficiency	ξ	100 [%]
Process variables	Mean work part radius	$\overline{R}_w$	8 [mm]
	Work part speed	N_w	95 [RPM]
	Tool eccentricity	e_t	2.25 [mm]
	Tool orbiting speed	N_t	0 [RPM]
	Feedrate of tool	f	0.01 [mm/s]
	Work part radius	$Rw(j,k)$	[mm]
	Change in part radius	$\Delta Rw(j,k)$	[mm]
	Voltage	V	20 [v]
	Volume removed	v_a	[mm3]
	Linear rate	LRR	[µm/min]
	Volumetric rate	VRR	[mm3/min]
	Average straight. error	SE_m	[µm]
	Total time	T	[min]
	Machining time	T	[Sec.]
	Segment current	I_s	[A]
	Total current	I_a	[A]
	Average radius change	ΔR_w	[mm]
	Gap	$g(l,k')$	[mm]
	Gap variations	$\Delta g(l,k')$	[mm]
	Machining power	W	[W]
	Specific cutting energy	W_s	[W.s/mm3]
	Average round. error	RE_m	[µm]
	Roundness error of disc	RE	[µm]
	Tool position	X	[mm]
	Straight. of hole side	SE	[µm]
Simulation parameters	Disc height	H	0.1 [mm]
	No. of work part discs	J	150 [ ]
	Number of tool discs	L	50 [ ]
	Time step	Δt	0.0002 [s]
	Equiv. eccentricity. angle	φ_q	[°]
	Equivalent eccentricity.	e_q	[mm]
	No. of segments	K	1000 [ ]

volt, tool position and incremental volumetric and linear removal rates are saved in a text file. If tool is still inside the hole, in case of a feeding tool, or time limit for machining, in case of cylindrical tool, is not exceeded, simulation time is incremented and simulation loops. Otherwise, simulation stops and final hole geometry, as represented by hole radius data structure, is saved in a text file. Then, straightness and roundness errors as well as over all volumetric and linear removal rates and average specific machining energy are calculated.

5. Simulation results and discussions

Fig. 3 shows the effect of tool radius R_t on specific cutting energy, W_s, volumetric and linear removal rates, *VRR and LRR*, and average roundness and straightness errors, RE_m, SE_m, for both feeding and non-feeding tools. From fig. 3-a, it can be seen that the effect of R_t on W_s is marginal. More importantly, the figure shows that the values of W_s for the OECHS process are much larger compared with those for conventional machining operations [17]. Also, the value of W_s for feeding and non-feeding tools are almost identical. This indicates that W_s is a process characteristic rather than a process performance measure.

Fig. 3-b shows that increasing R_t increases both *VRR and LRR*. Increasing R_t widen the tool conducting zone and consequently the work part machining zone, fig. 1. As a result, the amount of material removed per unit time increases and consequently values of *VRR and LRR*. The values of *VRR and LRR* are comparable with those for conventional machining operation, specially, for hard to machine materials.

Fig. 3-c shows that increasing R_t has no effect on SE_m for the case of the non-feeding tool, while increasing R_t decreases SE_m for the case of the feeding tool. The reason for this result is that; for the case of the non-feeding tool, the gaps $g(l,k')$ between the hole radial segments, having the same index k', and the tool are equal at any point of time for all hole discs. This results in no variations in the hole radius at these segments and consequently no straightness errors were simulated. However, this condition does not exist for the case of the feeding tool, where tool height is less than hole height, and consequently straightness errors develop.

The decrease in SE_m with the increase in R_t can be explained in light of the fact that increasing R_t decreases the variations in the gaps $g(l,k')$ within the machining zone and, consequently, more uniform machining takes place. This results in the reduced RE_m. In fact, this also explains the decrease in RE_m for both the feeding and non-feeding tools with the increases in R_t as shown in fig. 3-c.

Fig. 3-d shows incremental versus average W_s. From the figure, it can be seen that incremental W_s slightly increases over time. The increase of W_s is due to the increase in the machining gap upon machining and the consequent decrease in machining current and machining capacity of the process. The increase is slight as slight changes in radius are obtained in the sizing process.

Figs. 4-a, 4-b and 4-c show that increasing work part speed, N_w, has no effect on W_s, *VRR*, *LRR* , RE_m nor SE_m. This is expected as N_w affects only the indices of the mating radial segments as expressed by eqs. (2-6 and 8). Fig. 4-d shows the incremental and overall *VRR*. From the figure, it can be seen that incremental *VRR* decreases over time. This is due to the increase in the machining gap upon time and the consequent decrease in machining current and machined volume.

Fig. 5 describes the effect of the tool lip height h_t on different process performance measures. Fig. 5-a shows that, h_t has a minor effect on W_s. Increasing h_t slightly decreases W_s. Fig. 5-b shows that increasing h_t increases both *VRR and LRR*. This is due to the increase in the sized conducting zone of the tool and the machining zone on the hole. Fig. 5-c shows that increasing H_t increases RE_m but has subtle effect on SE_m. Fig. 5-d shows that there are variations in W_s when the tool enters and exits the hole. This is basically due to non-uniform machining as only part of the tools is involved in machining. However, when the tool is within the hole, uniform W_s is obtained.

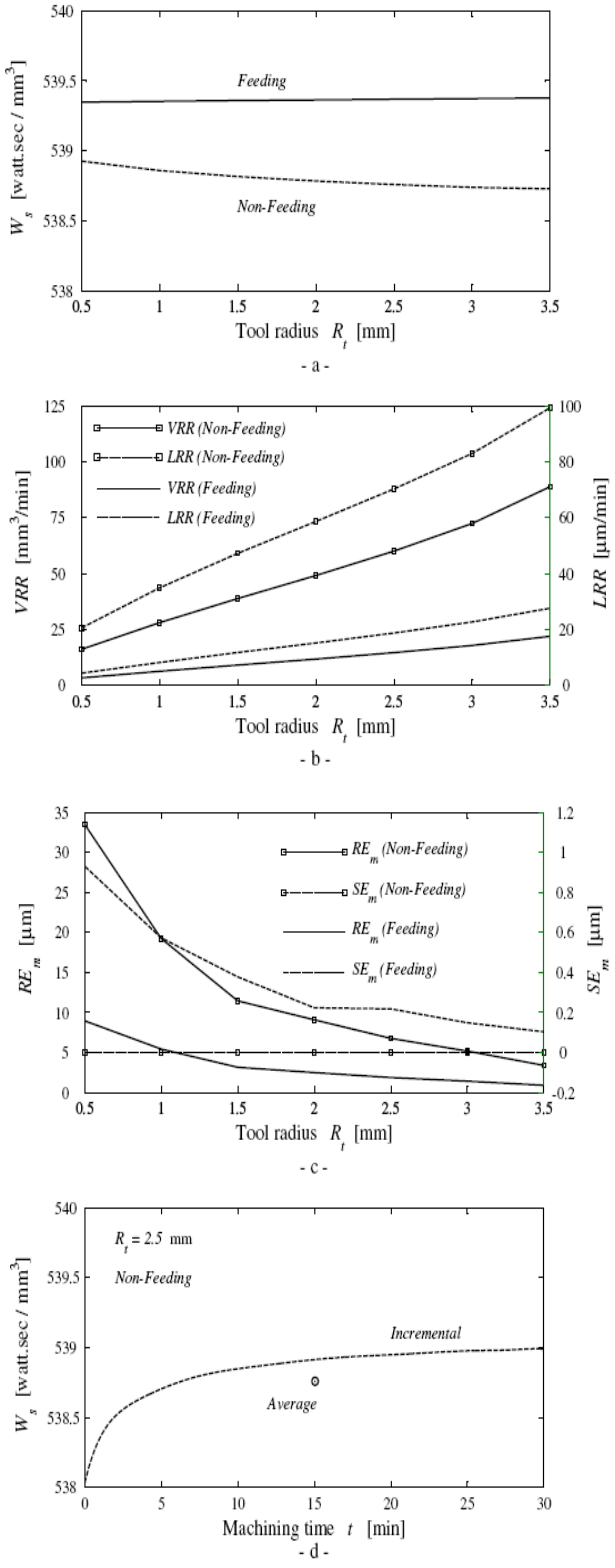

Fig. 3. Effect of tool radius R_t on different process performance measures.

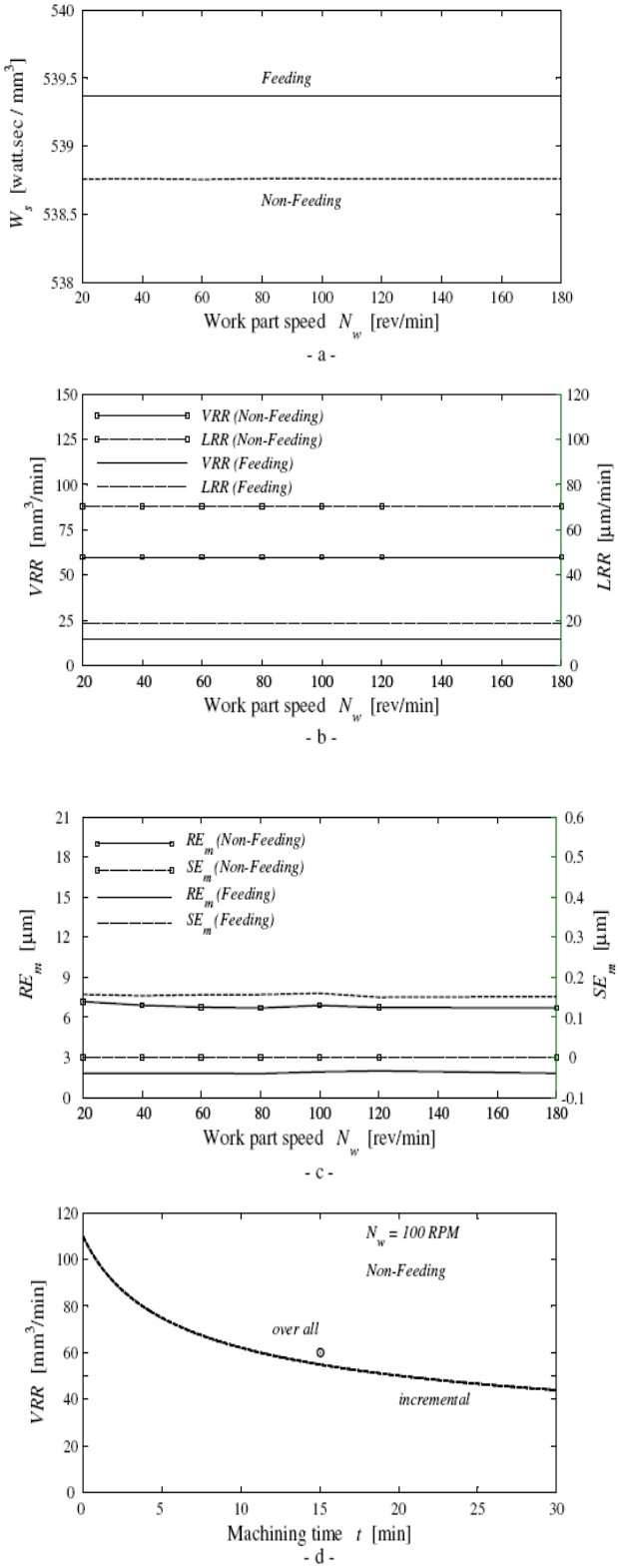

Fig. 4. Effect of work part rotational speed N_w on different process performance measures.

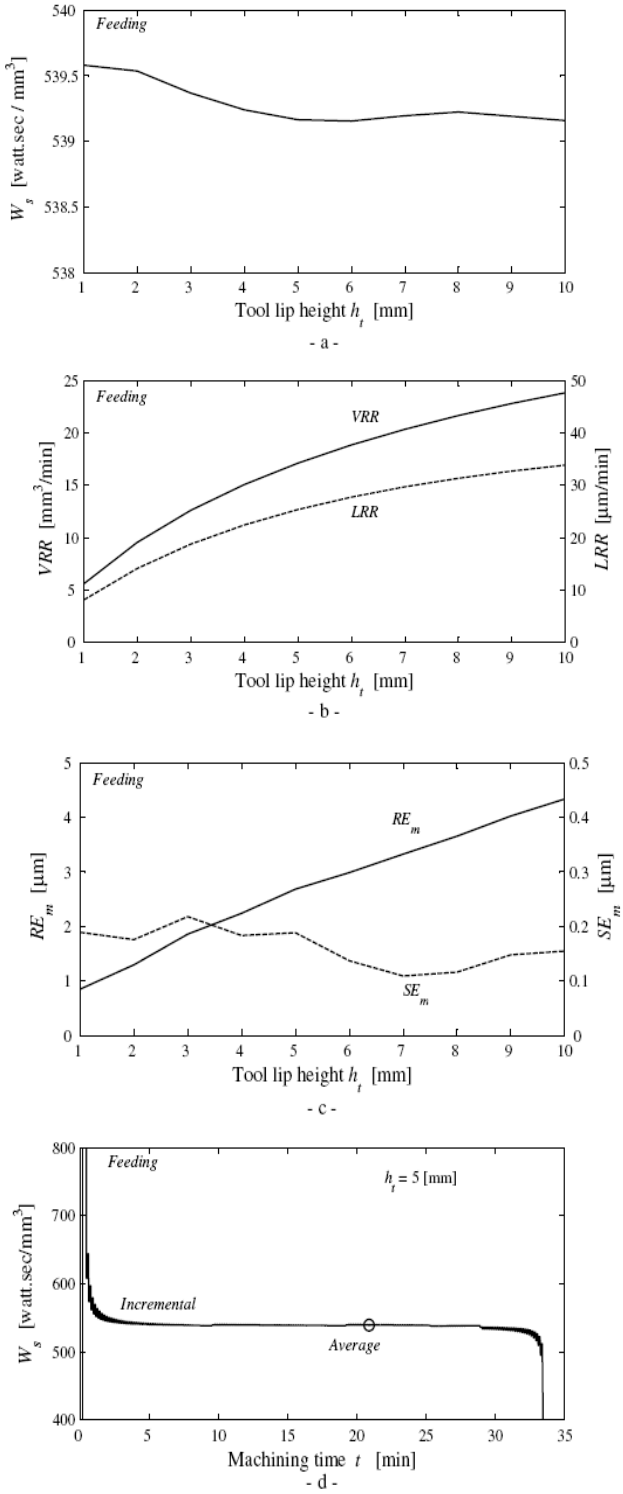

Fig. 5. Effect of tool lip height h_t on different process parameters.

Figs. 6-a and 6-b show the effects of the feedrate f on W_s, *VRR* and *LRR* respectively. From fig. 6-a it can be seen that f has small effect on W_s. Fig. 6-b shows that *VRR* and *LRR* slightly increase with the increase in f. This result favors sizing of a hole using several strokes at large feedrate over sizing the hole with one stroke at low feedrate. Fig. 6-c shows that increasing f decreases RE_m. This is due to the decrease in the amount of material removed and the consequent decrease in variations in the hole radius at each hole disc. The figure also shows that f has almost no effect on SE_m.

Fig. 7 shows the results of simulating the OECS process using a feeding tool with a constantly increasing feedrate. Fig. 7-a shows feedrate versus time. Fig. 7-b shows variations in machining current I_a over time. From the figure, it can be seen that I_a rapidly increases as the tool engages the hole. It also shows that I_a slightly increases while the tool is within the hole. This is because the increase in the feedrate does not allow large amount of material to be removed and consequently the minimum machining gap keeps close to its initial minimum value, $g(1,1)_{t=0}$. Fig. 7-c shows the variations in the average disc radius along hole axis. At the top of the hole, left side of the figure, average radius is relatively large due to the low feedrates. Fig. 7-d shows that for larger average disc radius, the value of *RE* is larger. Generally, the more material is removed, the more radius variations and consequently larger roundness error.

Figs. 8-a shows that work part eccentricity e_w has slight effect on W_s. Also, fig. 8-b shows that the increase in e_w has a minor effect on *VRR* and *LRR*. However, fig. 8-c shows that increasing e_w significantly increases RE_m. This is because the increase in e_w results in uneven machining from hole surface, especially in the radial direction. Increasing e_w also increases SE_m.

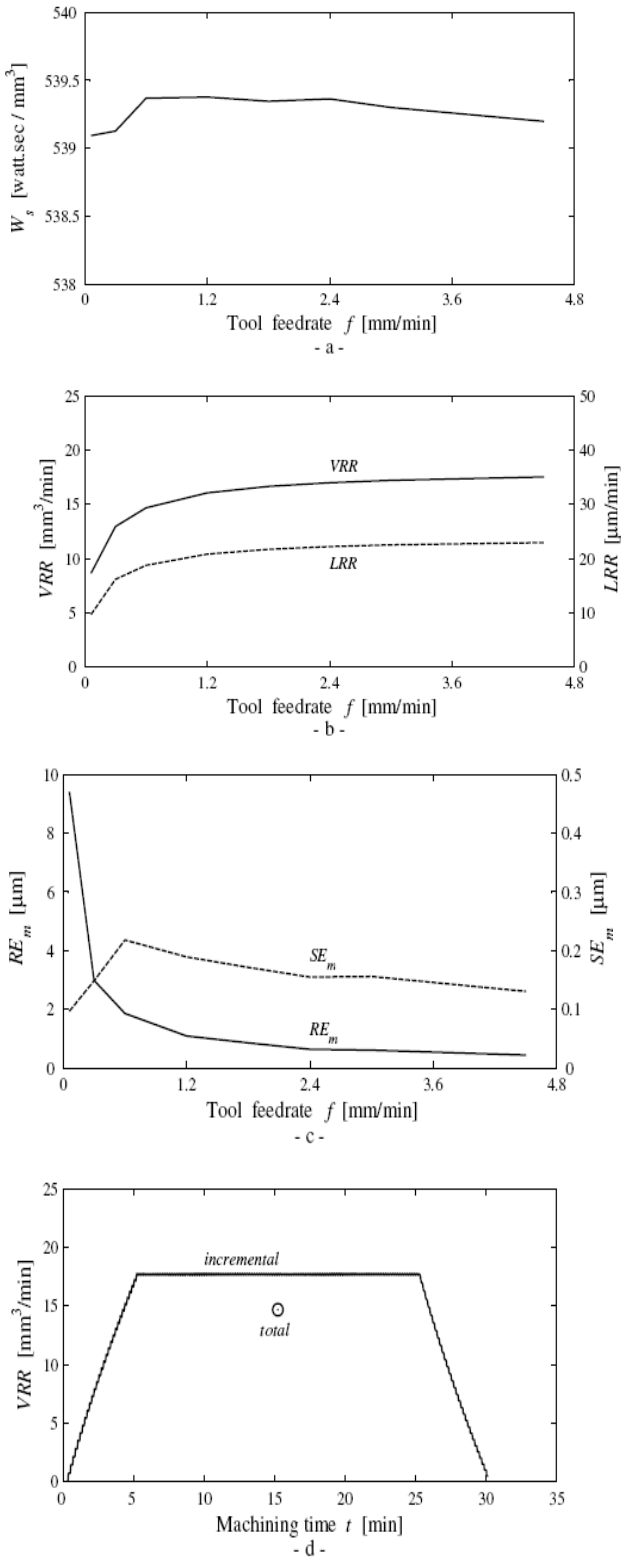

Fig. 6. Effect of feedrate f on different process performance measures.

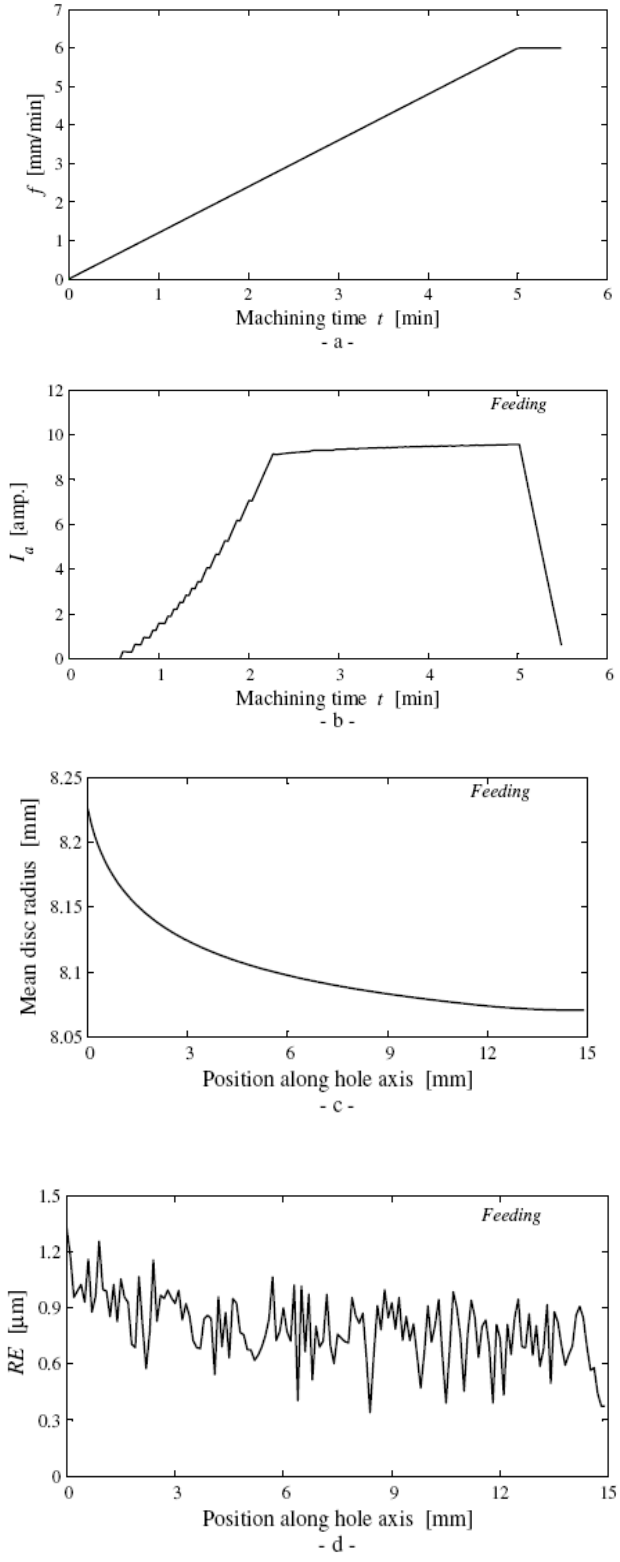

Fig. 7. Simulation results using a feeding tool with a linearly increasing feedrate.

Figs. 9-a shows the variations in machining current due to e_w of 0.3 mm. Fig. 9-b shows the current density distribution in the machining zone at different machining times. Current density distribution, at certain machining time, is determined at the work part disc facing the bottom disc of the tool. From the figure, it can be seen that at the middle of the machining zone, the current density has a maximum value, where the machining gap has its minimum value. Maximum current density varies due to work part eccentricity.

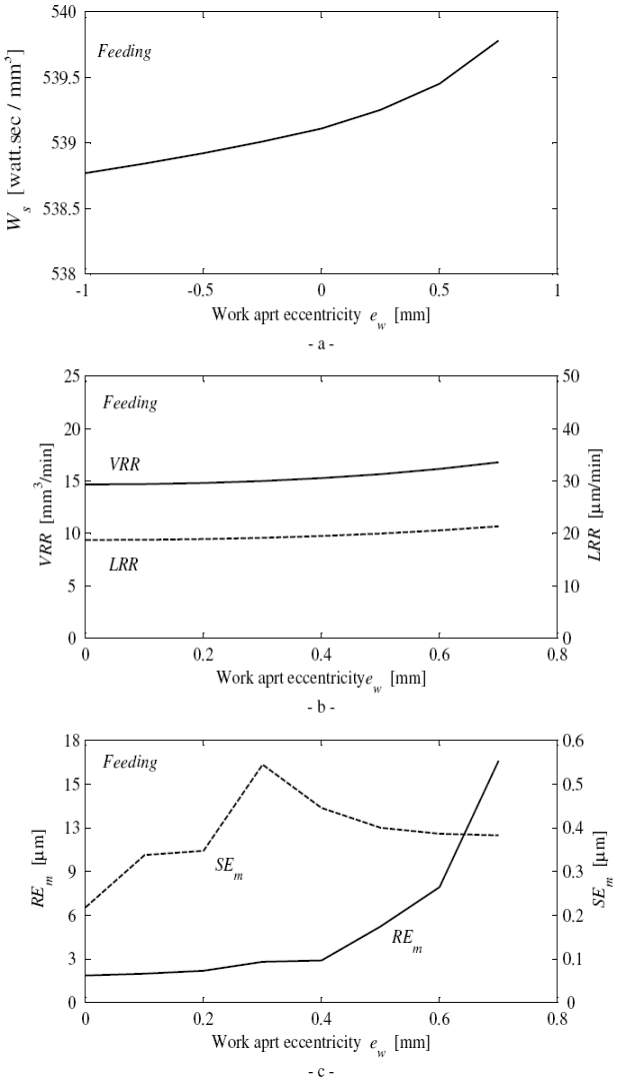

Fig. 8. Effect of work part eccentricity e_w on different process performance measures.

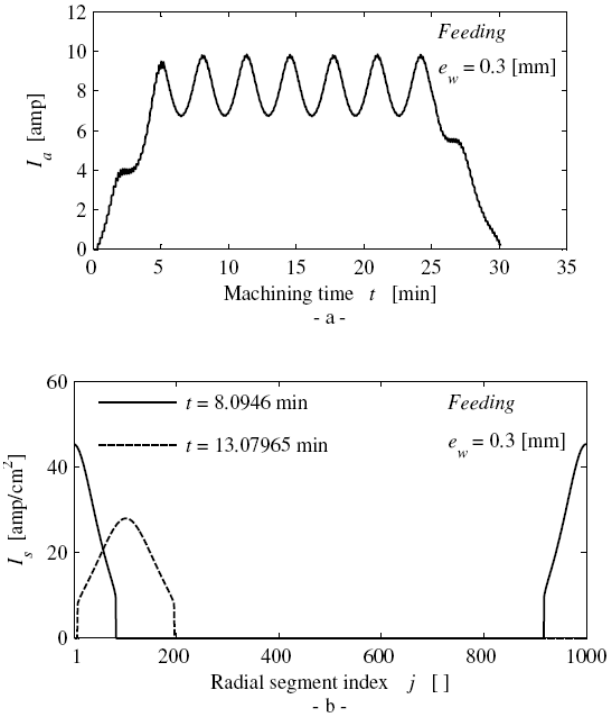

Fig. 9. Effect of work part eccentricity e_w on machining current and current density.

6. Conclusions

The developed model provides correlations between different process variables and parameters and process performance measures. Model simulations show that the rotational speeds of the tool and the work part do not affect process performance. Simulations, also, show that increasing tool radius, feedrate and tool lip height increases volumetric and linear removal rates and decreases mean straightness errors. Moreover, increasing tool radius and feedrate decreases hole average roundness error while increasing tool lip height increases it. The concepts of incremental and over all removal rates are introduced and compared. Incremental removal rates are more representative of process performance; however, the overall removal rates are more practical and easier to verify experimentally. Model simulations show that the specific cutting energy of the process is independent of process parameters, and its value is much larger compared with those for conventional machining operations.

References

[1] M. Shen and H.S. Shan, "A Review of Electrochemical Macro to Micro Hole Drilling", International Journal of Machine Tools and Manufacture, Vol. 45, pp. 137-152 (2005).

[2] M. Shen and H.S. Shan, "Analysis of Hole Quality Characteristics in the Electro Jet Drilling process", International Journal of Machine Tools and Manufacture, Vol. 45, pp. 1706-1716 (2005).

[3] J. Kozak, "Mathematical Models for Computer Simulation of Electrochemical Machining Processes", Journal of Material Processing Technology, Vol. 76, pp. 170-175 (1998).

[4] J. Kozak, A.F. Budzynski and P. Domanowski, "Computer Simulation Electrochemical Shaping (ECM-CNC) Using a Universal Tool Electrode", Journal of Material Processing Technology, Vol. 76, pp. 161-164 (1998).

[5] H. Hardisty, A.R. Mileham and H. Shirvani, "A Finite Element Simulation of the Electrochemical Machining Process", Annals of the CIRP, Vol. 42 (1), pp. 201-207 (1993).

[6] M. Purcar, L. Bortels, B.V. Bossche and J. Deconinck, "3D Electrochemical Machining Computer Simulation", Journal of Material Processing Technology, Vol. 149, pp. 472-478 (2004).

[7] H. Hocheng, P.S. Kao and S.C. Lin, "Development of Eroded Opening During Electrochemical Boring of Hole", International Journal of Advanced Manufacturing Technology, Vol. 25, pp. 1105-1112 (2005).

[8] H. Hocheng, Y.H. Sun, S.C. Lin and P.S. Kao, "A Material Removal Analysis of Electrochemical Machining Using Flat-end Cathode", Journal of Material Processing Technology, Vol. 140, pp. 264-268 (2003).

[9] X. Jiawen, Y. Naizhang, T. Yangxin and K. P. Rajurkar, "The Modeling of NC-Electrochemical Contour Evolution Machining Using a Rotary Tool-cathode", Journal of Material Processing Technology, Vol. 159, pp. 272-277 (2005).

[10] M.S. Hewidy, S.J. Ebeid, K.P. Rajurkar and M.F. El-Safti, "Electrochemical Machining Under Orbital Motion Conditions", Journal of Material Processing Technology, Vol. 109, pp. 239-346 (2001).

[11] K.P. Rajurkar and D. Zhu, "Improvement of Electrochemical Machining Accuracy by Using Orbital Electrode Movement", Annals of the CIRP Vol. 48 (1), pp. 139-142 (1999).

[12] H. El-Hofy, N. Al-Salem and M. Abd-ElWahed, "Orbital Electrochemical Finishing of Holes Using Stationary Tool", CAPE-10, 18-19 March, Edinburgh, Scotland, pp. 169-177 (2003).

[13] N. Al-Salem, H. El-Hofy and M. Abd-ElWahed, "Orbital Electrochemical Hole Finishing Using Feeding Tools", Al-Azhar Engineering 7th International Conference 7-10 April (2003).

[14] E. Soliman and H. El-Hofy, "Electrochemical sizing of through holes"; International Conference on Advances in Manufacturing and Technology Management, Parshvanath College of Engineering, Thane (W) Mumbai, Maharashtra, India, January 18-20 (2007).

[15] E. Soliman and H. El-Hofy, "Modeling and Experimental Investigation of the Electrochemical Hole Sizing Process", Alexandria Engineering Journal, Vol. 46 (6), pp. 797-809 (2007).

[16] J.F.W. Galyer, and C.R. ShotBolt, "Metrology for Engineers", Cassell Publishers Ltd, Villiers House, 41-47 Strand, London, WC2N 5JE, ISBN 0 304 31734 9 (1990).

[17] S. Kapakjian and S.R. Schmid, "Manufacturing Processes for Engineering Materials", International Edition, 4/E, Prentice Hall, ISBN-13 9780130453730 (2003).

[18] A.D. Davydov, V.M. Volgin and V.V. Lyubimov, "Electrochemical Machining of Metals: Fundamentals of Electrochemical Shaping", Russian Journal of Electrochemistry, Vol. 40 (12), pp. 1438-1480 (2004).

Received July 30, 2007
Accepted January 29, 2008